Journal of the Nigerian Association of Mathematical Physics
Volume **23 (March, 2013), pp 153 – 164**

Radio Frequency Power Dissipation with Contribution from Flowing Blood in Human Patient Undergoing NMR/MRI

[1]Odoh, Emmanuel O and [2]De, Dillip K
[1]Department of Physics,
Modibbo Adama University of Technology,
[2]Department of Physics,
Kaduna State University, Kaduna – Nigeria Abstract

Abstract

A new look has been given to the problem of radiofrequency (rF) power absorption inherent in all NMR/MRI scanning instruments. In the present approach, we have considered for the first time the contribution of flowing blood to rF power absorption. Our result shows that flowing blood spin contribute to a good degree to the power losses - both Faraday power loss, P_f, and the electrostatic capacitance power loss, $P_C$especially low frequency fields. For efficient NMR coil design, the ratio P_C/P_fisone of the most important factors that should be known. Computations based on our algorithm showed that the variations of P_C/P_f with the patient length (L_0), the proximity of the patient to the capacitor plate (L), electrical conductivity (σ_t) at electrical conductivity of blood of 0.0054 s/m satisfy the condition $P_C/P_f << 1$. This indicates therefore, that rF absorption in the patient has important contribution fromflowing blood spin in the tissue and such contribution should be taken into account in NMR instrument design for the purpose of medical diagnosis.

Keywords: Radiofrequency, Power dissipation, Blood flow, Magnetic Resonance, Imaging.

1.0 Introduction

Nuclear magnetic resonance has been established of molecules, molecular motion, rate processes and molecular interactions. Daily use of this technology results in the exposure to both static and time varying fields. Patient exposure to high intensity electric and magnetic fields is likely to increase with the development of high field imaging systems, fast cardiac imaging methods and localized magnetic resonance spectroscopy [1]. In addition to patient exposure, the development of intervention MR-guided procedures and open magnet structure will substantially increase the exposure of physicians and medical workers. The development of 3T and 4T MRI systems that employ more intense fields should be studied carefully to determine their potential biological effects (especially sensitive biological systems). Such field condition may produce biological effects that are not observed with the current generation of clinical imaging systems.

In this the total rF power loss, p, inside a patient undergoing magnetic resonance imaging (MRI) examination warrants careful study at least a theoretical consideration because of the following reasons:

(i)Fast changes in magnetic field, which occur during gradient switching, causing
Faraday current in tissue. The most sensitive tissue to this current is the retina, which can be activated, resulting in flash-like sensations.

(ii)The MR pulses used in MR imaging produces warming of the tissues. This could result in local thermal injury which may cause thermal overload with an extra burden on the vascular system. rF heating increases with square of the B_1 field strength since the absorbed energy is roughly proportional to the square of the rF used.

(iii) In medical physics, the amount by which the body temperature can be allowed to rise depends on this power loss and it is strictly limited [2-5] so that the biological functions of the patient's body would not be adversely affected.

(iv) The characteristics of the isolated coil, electric and magnetic field interactions within the patient, determine the magnetic resonance (MR) receiver coil limiting performance.

The MR receiver limiting performance depends strongly upon the rF power loss, P, together with the rF power loss in the isolated MR coil. The total power loss p, is a summation of two factors: (1) rF power loss P_f due to Faraday induction electric field, E_f, induced by the rF B_1 field inside the patient body according to the Maxwell's equation;

$$\nabla \times E_f = -\frac{\partial B}{\partial t}$$

and (2) the rF power loss, P_c, due to the "Electrostatic coulomb's law electric field, E_c" inside the patient. E_c is produced by charge distribution on the NMR coil windings and can be identified with the distributed capacitance along the rF coil and some stray capacitances.

Corresponding author: ***Odoh E. O.,*** E-mail: odophfy@yahoo.com-, Tel. +234 7061268101

For a given MR imaging sequence, the Faraday induction power loss, P_f is unavoidable, whereas the capacitive field loss, P_c can be minimized depending on the subject coil relationship [6] and coil design properties. Besides increasing the total power deposition in biological tissues, P_c can also contribute to the noise of the MRI signal.

Knowledge of these two losses and the subject/coil relationships (during actual MR sequences for medical imaging) will help us to understand some fundamental coil design properties especially when human patients are subjected to MRI [2-4], to electromagnetic fields and radiations [1, 7-13].

The results of [14] had earlier shown that the exposure of the uterus of a mice to a high field (4.7 T), long duration (8h) MRI alone and in combination with ultrasound exposure (MHz, CW, 5W/cm^2 unfocussed) reduced fetal growth, neonatal survival, and male reproductive development when it occurred during sensitive times of the developmental cycle, and that some of the effects were permanent. Considering the volume of work listed above, the growing interest and importance of the knowledge of exact effects of the rF power deposition in the human tissue cannot be over emphasized.

Much as the Faraday's induction electric field loss in a patient subject placed in MRI instrument depends much on the electrical conductivity of the subject, more recent studies have also focused on the estimation of the electrical conductivity of the human tissue. It has been shown [15] that electrical conductivity of a tissue is inhomogeneous on a microscopic scale but on a macroscopic scale the conductivity can be considered to be homogenous. The electrical conductivity of a flowing blood has also been shown by [16] to depend on the flow velocity. He also explained that if blood flows through a cylindrical tube, shear stresses will deform and align the red blood cells with one of their long axes parallel to the stream lines. The pathway of a low-frequency (> 1 MHz) alternating electrical current will be altered by this orientation and deformation of the red blood cells. Consequently, the electrical conductivity in the flow direction of blood increases. We have derived theoretical expressions for P_c and P_f based on a simple model of the subject/coil system. We have considered the patient to be uniform cylinder having spatially uniform (isotropic) dielectric with dielectric constant, K, and electrical conductivity σ, of the tissue in the first. The contribution of the flowing blood to these power loses in the case of the isotropic conductivity has been clearly presented.

2.0 Theory

The rF voltage across NMR coil generates a magnetic field vector B_1 which in turn stimulates NMR. This voltage gives rise to two types of electric field:

(i) A conservative field or electrostatic field, E_c that obeys the Maxwell's equations

$$\left.\begin{aligned} \nabla . E_C &= \frac{\rho}{\varepsilon_0} \\ \nabla \times E_C &= 0 \end{aligned}\right\} \quad (1)$$

(ii) The non-conservative field or Faraday field $E_{f,}$ that obeys Maxwell's equation

$$\nabla \times E_f = -\frac{\partial B_1(t)}{\partial t} \quad (2)$$

E_c in the NMR coil is produced by charge distribution on the coil windings and can be identified with the distributed capacitance along the rf coil. The total field E inside the patient is given by

$$E = E_C + E_f \quad (3)$$

To calculate the loses P_C and P_f, [17], considered a model which the patient was assumed to be a uniform cylinder of length L_0 and cross-section Ω_p, and was inside a curved capacitor plates (which are parallel to the rf coil) such that the cylinder surfaces were at distance L/2 from the plates as in Fig. 1. His model was also applicable to the case where the patient (a uniform cylinder of length L_0) was placed symmetrically around the coil axis; the end being at distance L/2 from the physical coil ends (Fig. 2). In this latter model, it was assumed that all the distributed and stray capacitances are replaced by two capacitances at the ends of the coil. The rf voltage V_0, occurs across the capacitor plates generates the rf electric field, E_c, which is parallel to the length of the cylinder. In either case L/2 is a parameter that determines the proximity of the skin to the rf coil surfaces or ends.

To estimate the stray-capacitance power dissipation, $P_{c,}$ he used the Maxwell's equations (1) considering the patient as a conducting medium having an isotropic conductivity σ. Consequently, from Maxwll's equation

$$\nabla \times \mathrm{B}_1 = \mu_0 j + \mu_0 \varepsilon_0 k \frac{\partial E}{\partial t} \quad (4)$$

$$E = E_0 e^{j(\omega t + \theta)} \quad (5)$$

$$j = \sigma E \quad (6)$$

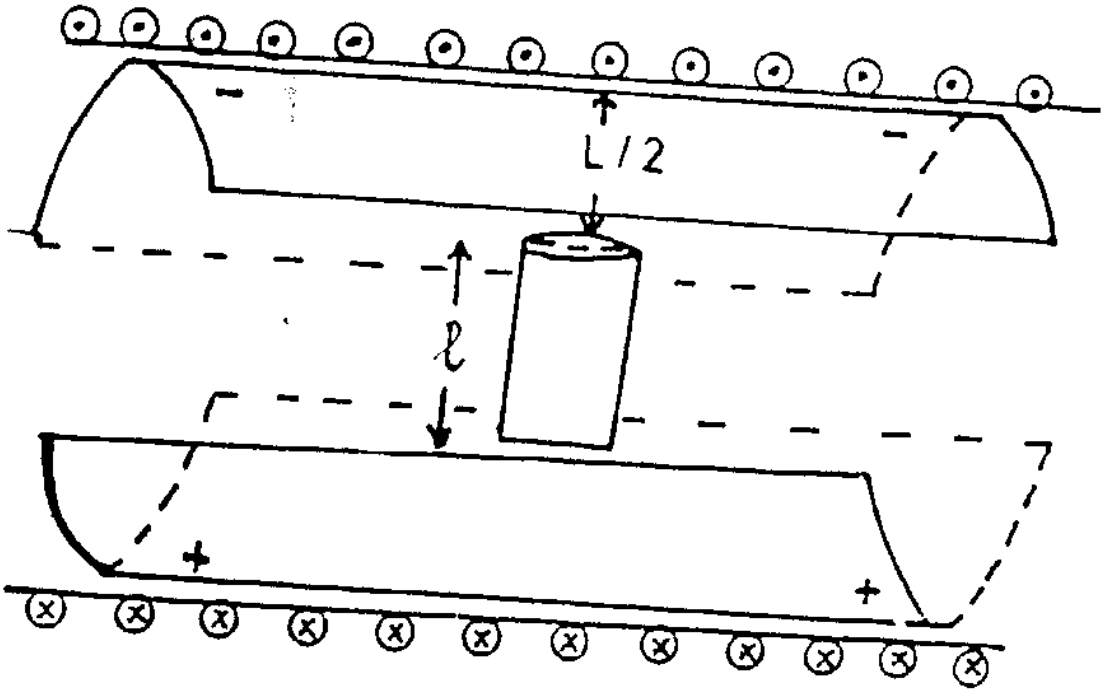

Fig 1 Two cylindrical curved (charged) surfaces with the Subject symmetrically placed such that the curved surfaces are at a distance of L/2 from the surface of the subject cylinder.

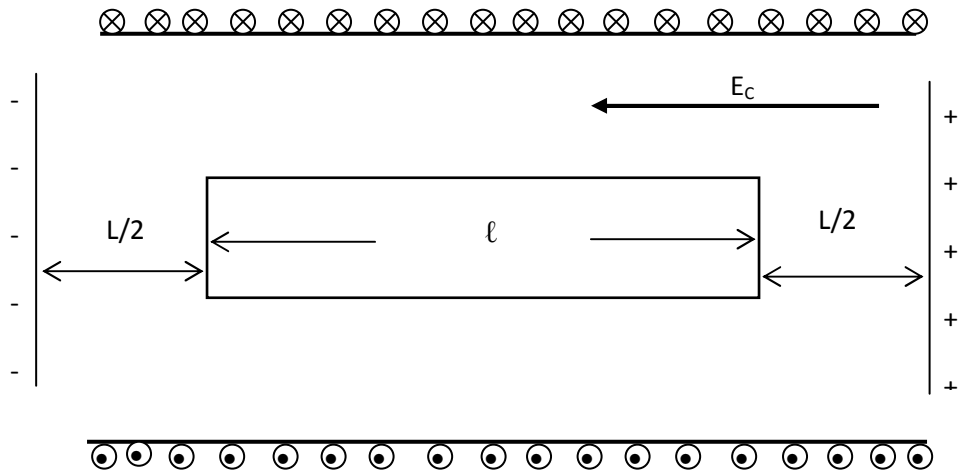

Fig. 2 Two Parallel Plates such that the Plates are at a Distance of L/2 from the extreme of the Subject/Cylinder.

Assuming current density j within the patient body arises solely due to the rF electric field and finite electrical conductivity, equation (4) could then be written as

$$\left.\begin{aligned} \nabla \times B_1 &= \mu_0 \sigma E + \mu_0 \varepsilon_0 ki\, \omega E \\ \nabla \times B_1 &= \mu_0 \varepsilon_0 k_{eff} \frac{\partial E}{\partial t} \end{aligned}\right\} \quad (7)$$

Thus effective (phase) dielectric constant, K_{eff}, due to finite conductivity σ, of the sample or patient tissue, which is frequency independent over a 0-100 MHz for saline solution [18] in the presence of the rF field of frequency, $\omega/2\pi$, is given by

$$keff = k\left(1 - \frac{i\sigma}{\varepsilon_0 \omega k}\right) \tag{8}$$

Assuming the patient to have uniform electric constant, k, P_C and P_f can be expressed as

$$P_C = \tfrac{1}{2} \int_{patient} \sigma E_C E_C^{\,*} dv \tag{9}$$

$$P_f = \tfrac{1}{2} \int_{patient} \sigma E_f E_f^{\,*} dv \tag{10}$$

where $E_C^{\,*}$ and $E_f^{\,*}$ are the respective complex conjugates of E_C and E_f.

Equations (9) and (10) were arrived at from the following assumptions.

(i) The skin depth is much larger than the sample dimension.

(ii) The coil is operated at frequencies well below self-resonance so that the current is always uniformly distributed in the coil windings.

(iii) The coil with the patient is not in self resonant mode

In the case, where the skin depth d is smaller than the sample dimensions, equations (9) and (10) are given by

$$P_c = \tfrac{1}{2} \int_{x=0}^{L_0} \int_{0}^{R} \sigma E_C E_C^{*} 2\pi r dr dx \tag{11}$$

$$P_f = \tfrac{1}{2} \int_{x=0}^{L_0} \int_{R-d}^{R} \sigma E_f E_f^{*} 2\pi r dr dx \tag{12}$$

where R is the radius of the cylinder and d, the skin depth, is given as

$$d = 2\left(2\omega\mu\sigma\right)^{\frac{1}{2}} \tag{13}$$

Since the ratio of P_c/P_f gives a clue to designing efficient MRI/CW NMR coils, Awojoyogbe focused attention on equations (9) and (10). The rF voltage, V_0, appearing on the capacitor plate was given as

$$V_0 = E_0\left(\frac{L}{2} + \frac{L}{2}\right) + E_C L_0$$

where $E_C = \dfrac{E_0}{k_{eff}}$

$V_0 = k_{eff} E_C L + E_C L_0$, so that

$$E_C = \frac{V_0}{L_0 + k_{efff}} \tag{14}$$

E_C and E_0 are the rF electric field inside the patient and that of the space between the patient and the coil respectively. With equation (14), (9) becomes

$$P_C = \frac{1}{2} \int_{patient} \frac{\sigma V_0 \bullet V_0}{\left(L_0 + k_{eff} L\right)\left(L + k_{eff}^{*}\right)} dv \tag{15}$$

With an assumed σ and k spatially uniform throughout the patient, equation (15) becomes

$$P_C = \frac{\sigma V_0^{\,2} \Omega_p L_0}{2\left(L_0^2 + 2LkL_0 + L^2 k^2\right) + \dfrac{L^2 \sigma^2}{\varepsilon_0^2 \omega^2}} \tag{16}$$

where Ω_P is the cross-section of the patient-cylinder; $\Omega_P L_0$ is therefore the patient's volume.

The rF B_1 field which stimulates the MRI signal is generated by the current in the excitor as a result of full external voltage V_0, appearing on the coil. The inductive energy of the coil equals the circulating energy due to the rF B_1 field and therefore

$$\frac{1}{2\mu_0}\int B_1^2 dv = \frac{1}{2}L_i I^2 \qquad (17)$$

where $L_i$is the self inductance of the excitor (after being loaded in the coil. I is related to V_0 by the relation

$$V_0 = Z_c I = I\omega L_i ,$$

Z_C beingthe impedance of the coil seen at the input terminal when the patient is undergoing MRI sequence. Z_C is different from the impedance, Z_0, of the coil (at the same frequency) in the absence of the patient. Then equation (16) becomes

$$P_C = \frac{\sigma\omega^2 L_i^2 I^2 \Omega_p L_0}{2\left(L_0^2 + 2LkL_0 + L^2k^2\right) + \dfrac{L^2\sigma^2}{\varepsilon_0^2\omega^2}} \qquad (18)$$

The inductive energy is

$$U = \int L_i I dI = \frac{1}{2}L_i I^2 .$$

Then equation (18), using equation (17) gives

$$P_C = \frac{C_0 F_C \Omega_C \omega^2 \sigma}{2\mu_0}\int_{coil} B_1^2 dv \qquad (19)$$

where $C_0 = \dfrac{L_0 L_i}{\left(L_0^2 + 2LkL_0 + L^2k^2\right) + \dfrac{L^2\sigma^2}{\varepsilon_0^2\omega^2}}$

and

$$F_C = \frac{\Omega_P}{\Omega_C} \qquad (20)$$

Equation (20) gives the filling factor of the instrument.

The rF power loss, P_C, due to the electrostatic coulomb electric field, E_C inside the patient calculated above by Awojoyogbe clearly shows that it is the contribution from only the static tissue. However, along with the static tissue contribution, there must certainly be a corresponding rF power loss as a result of flowing spin in the blood when the patient is subjected to an MRI/CW NMR scan. Such loss cannot be neglected as the excitation of the flowing blood spins that actually bring about flow dependent NMR signal. It is therefore a fact that equation cannot be said to precisely account for the rF electrostatic power loss as has been presented above. Knowing that the electrical conductivity of the blood varies with the velocity [16] we therefore present a more accurate theory to quantitatively account for this loss arising from the blood velocity.

3.0 Contribution Of Flowing Blood To rF Power Loss In Human Tissue

To account for the rF power in human and show clearly that the flowing blood also contribute to the power absorption, we shall consider the vessel to be a cylindrical tube as shown in Fig. 3. Suppose the blood is flowing in a vessel of radius, r; dr represents change in the cross-section of the vessel. As the vessel is excited by an rF pulse an electric field E_f is created by I so that along the inside of the vessel we have the field of which the radial field passes axially through the vessel.

The radio-frequency power absorbed per unit volume by the tissue and the blood in the vessel is given by

$$\frac{\sigma E_f E_f^*}{2} = \frac{E_f^* J_f}{2} \qquad (21)$$

where σ is the electric conductivity of the patient which can still be considered the same in all parts of the tissue (isotropic case). J_f is assumed as the current density within the patient arising solely due to rF electric field and finite conductivity of the blood. Clearly,

$$J_f = \sigma E_f \qquad (22)$$

If the length of the section of the vessel length through which the blood flows is dl, then the total power loss with this section is $\dfrac{\sigma E_f E_f^*}{2}.2\pi r dr dl$.

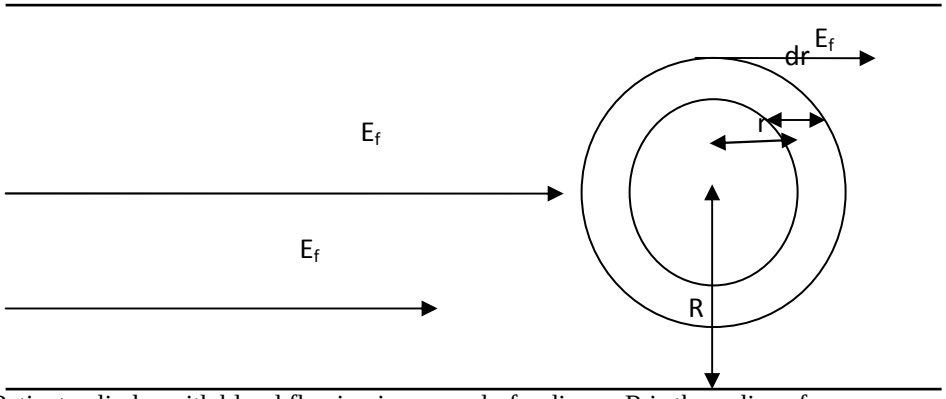

Fig 3 Patient cylinder with blood flowing in a vessel of radius, r. R is the radius of the cylinder and E_f is the induced Faraday field.

Let J_f° be the induced current density by the $E_f$field where

$$J_f^0 = nev_d \tag{23}$$

The total current density with the contribution from the flowing blood will be

$$J_f = ne\left(v_d + \langle v \rangle\right) \tag{24}$$

where n is the total number of induced charges caused by the rF field, e is the charge. v_d and $\langle v \rangle$ denote the drift velocity of current carriers in static blood and average blood flow respectively. From equation (24)

$$\left(J_f\right)_{total} = ne\left(v_d + \langle v \rangle\right) + J_{f_2}^0$$

$$= J_f^0\left(1 + \frac{\langle v \rangle}{v_d}\right) + J_{f_2}^0$$

which can be written as

$$\left(J_f\right)_{total} = J_{f_1}^{o}\left(1 + \frac{\langle v \rangle_{blood}\, m_p}{e\,\tau E}\right) + J_{f_2}^{0} \tag{25}$$

$v_d = \dfrac{e\tau E}{m_p}$, $J_f^0 = J_{f_1}^0$, m_p = mass of proton , $E = E_f$ and τ is the drift time of the charge carriers in blood.

The first two terms of equation (25) represent the current density contribution from the flowing blood while the second, $J_{f_2}^0$ represents that of the tissue.

Considering now the contribution to power due to the current density $J_{f_1}^0$ and $J_{f_2}^0$ arising in the patient volume $2\pi rdrdl$ as given by the patient cylinder in the figure above
and that due to flowing blood, per unit patient volume

$$P\left(J_{f_1}^0\right) = \sigma_b E_f E_f^*$$

$$P\left(J_{f_2}^0\right) = \sigma_t E_f E_f^* \tag{26}$$

Since the total current flowing in the conductor is made of the two components, we can write that

$$J = J_{f_1}^0 + J_{f_2}^0 \tag{27}$$

The total Faraday power absorbed by the patient now become

$$P_f = \int_{\substack{overblood\\volume}} \sigma_b E_f E_f^*\left(1 + \frac{\langle v \rangle m_p}{e\,\tau E_f}\right) 2\pi rdrdl + \int_{\substack{overtissue\\volume}} \sigma_t E_f E_f^* 2\pi rdrdl \tag{28}$$

The flow of blood through the vessel is laminar but parabolic. Therefore considering the axial velocity of the blood to be v_0, (Fig. 4) its effective value is reduced as one considers the progress, *a* from the centre of the vessel to its wall. The radial velocity is therefore given as

$$v(r) = v_0\left(1-\frac{r^2}{a^2}\right) \tag{29}$$

where *r* is the blood vessel radius.

To evaluate equation (28), we consider that the Faraday electric field at any radius, r is

$$E_f = i\omega B_1 r \tag{30}$$

This means the rF B_1 field should be applied in the direction of the y-axis of the (x,y,z) plane so that the current density goes in the direction of the patient (x-axis) and

$$B_1 = B_1(r) \tag{31}$$

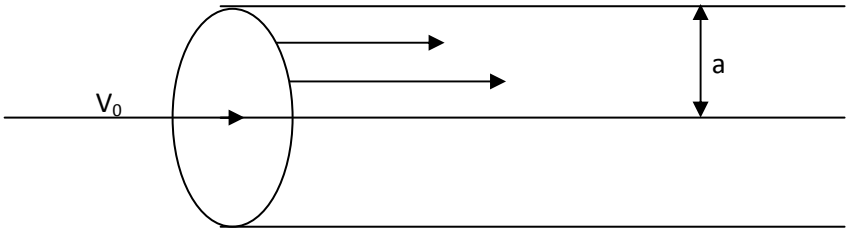

Fig 4 Parabolic laminar flow with axial velocity v_0 of blood in the vessel.

Evaluation of equation (28) can be tackled if $B_1(r)$ is replaced by average of $B_1(r)$ over the patient, so that

$$E_f = i\omega\langle B_1\rangle r \tag{32}$$

$$\langle B_1\rangle = \frac{1}{V_P}\int B_1(r)2\pi r\,dr\,dl$$

where V_P = patient volume subjected to NMR/MRI.

Using equation (32), equation (28) becomes

$$P_f = \int_{\substack{overblood\\volume}} \sigma_b\omega^2\langle B_1\rangle^2 r^2\left(1+\frac{\langle v\rangle m_P}{e\tau E_f}\right)2\pi r\,dr\,dl + \int_{\substack{overtissue\\volume}} \sigma_t\omega^2\langle B_1\rangle^2 r^2\,2\pi r\,dr\,dl \tag{33}$$

Considering now the tissue and vessel radii as given in Fig 3, equation (33) becomes

$$P_f = \omega^2\langle B_1\rangle^2\left[\sigma_b\int_0^a r^2.2\pi r\,dr + \sigma_t\int_a^R r^2.2\pi r\,dr + \int_0^a r^2\frac{\sigma_b m_P}{e\tau|E_f|}v_0\left(1-\frac{r^2}{a^2}\right).2\pi r\,dr\right]L_0$$

$$= \omega^2\langle B_1\rangle^2\left[2\pi\sigma_b\int_0^a r^3dr + 2\pi\sigma_t\int_a^R r^3dr + 2\pi\int_0^a \frac{r^3\sigma_b m_P v_0}{e\tau\omega\langle B_1\rangle}\left(1-\frac{r^2}{a^2}\right)dr\right]L_0 \tag{34}$$

$|E_f|$ = average Faraday electric field and L_0 is the patient length. Equation (34) can simply be integrated to give

$$P_f = \omega^2\langle B_1\rangle^2\left[2\pi\sigma_b\frac{r^4}{4}\Big|_0^a + 2\pi\sigma_t\frac{r^4}{4}\Big|_a^R + 2\pi\int_0^a\frac{\sigma_b m_P v_0}{e\tau\omega\langle B_1\rangle}\left(r^2-\frac{r^4}{a^2}\right)dr\right]L_0$$

$$= \omega^2 \langle B_1 \rangle^2 \left[\frac{\pi a^4 \sigma_b}{2} + \frac{\pi \sigma_t \left(R^4 - a^4 \right)}{2} + \frac{2\pi \sigma_b m_P v_0}{e\tau\omega \langle B_1 \rangle} \left(\frac{r^3}{3} - \frac{r^5}{5a^2} \right) \Big|_0^a \right] L_0 \quad (35)$$

which finally gives the Faraday loss as

$$P_f = \omega^2 \langle B_1 \rangle^2 \left[\frac{\pi a^4 \sigma_b}{2} + \frac{\pi \sigma_t \left(R^4 - a^4 \right)}{2} + \frac{4\pi \sigma_b m_P v_0 a^3}{15 e\tau\omega \langle B_1 \rangle} \right] L_0 \quad (36)$$

In all these derivations above, we have neglected the skin effect. This means a low frequency NMR should be used in this case. The above equation (36) shows that P_C depends on $\sigma_b, \sigma_t, a, R, V_0, \omega, \langle B_1 \rangle$ and τ. Thus V_0 is seen to influence the rF power loss in patient undergoing NMR/MRI.

4.0 Estimating The Stray-Capacitance Power Dissipation, P_c

The stray-capacitance power dissipation is exactly the same as presented by equation (28) except that the E_f is replaced by E_C as given in equation (14). Therefore we can write

$$P_C = \int_{\substack{overblood \\ volume}} \sigma_b E_C E_C^* \left(1 + \frac{\langle v \rangle m_P}{e\tau E_C} \right) 2\pi r dr dl + \int_{\substack{overtissue \\ volume}} \sigma_t E_C E_C^* 2\pi r dr dl \quad (37)$$

According to equation (14), $E_C = \dfrac{V_0}{L_0 + k_{eff} L}$ where all symbols have the same meaning as defined before, equation (37) becomes

$$P_C = \int_{\substack{overblood \\ volume}} \frac{\sigma_b V_0 \bullet V_0}{\left(L_0 + k_{eff} L \right)\left(L_0 + k_{eff}^* \right)} \left(1 + \frac{\langle v \rangle m_P}{e\tau E_C} \right) 2\pi r dr dl + \int_{\substack{overtissue \\ volume}} \frac{\sigma_t V_0 \bullet V_0}{\left(L_0 + k_{eff} L \right)\left(L_0 + k_{eff}^* \right)} 2\pi r dr dl \quad (38)$$

On inserting the expression for $\langle v \rangle$ and factoring, equation (38) results as

$$P_C = \frac{2\pi V_0 \bullet V_0 L_0}{\left(L_0 + k_{eff} L \right)\left(L_0 + k_{eff}^* L \right)} \left[\sigma_b \int_0^a r dr + \sigma_t \int_a^R r dr + \sigma_b \int_0^a \frac{m_P v_0 r}{e\tau \left(\dfrac{V_0}{L_0 + k_{eff} L} \right)} \left(1 - \frac{r^2}{a^2} \right) dr \right] \quad (39)$$

On simplifying equation (39), we have

$$P_C = \frac{2\pi V_0 \bullet V_0 L_0}{\left(L_0 + k_{eff} L \right)\left(L_0 + k_{eff}^* L \right)} \left[\sigma_b \int_0^a r dr + \sigma_t \int_a^R r dr + \frac{\left(L_0 + k_{eff} L \right) m_P v_0}{e\tau V_0} \sigma_b \int_0^a \left(r - \frac{r^3}{a^2} \right) dr \right] \quad (40)$$

which on integration using the same limits of integration as before gives

$$P_C = \frac{2\pi V_0 \bullet V_0 L_0}{\left(L_0 + k_{eff} L \right)\left(L_0 + k_{eff}^* L \right)} \left[\sigma_b \left(\frac{r^2}{2} \Big|_0^a \right) + \sigma_t \left(\frac{r^2}{2} \Big|_0^R \right) + \frac{\left(L_0 + k_{eff} L \right) m_P v_0 \sigma_b}{e\tau} \left(\frac{r^2}{2} - \frac{r^4}{4a^2} \right) \Big|_0^a \right]$$

Inserting the limits will result as

$$P_C = \frac{2\pi V_0 \bullet V_0 L_0}{\left(L_0 + k_{eff} L \right)\left(L_0 + k_{eff}^* L \right)} \left[\frac{\sigma_b a^2}{2} + \frac{\sigma_t R^2}{2} + \frac{\left(L_0 + k_{eff} L \right) m_P v_0 \sigma_b a^2}{4 e\tau V_0} \right] \quad (41)$$

which is simplified as

$$P_C = \frac{2\pi V_0^{\,2} L_0}{\left(L_0^{\,2} + 2L_0 kL + L^2 K^2\right)}\left[\frac{\sigma_b a^2}{2} + \frac{\sigma_t R^2}{2} + \frac{\left(L_0 + k_{eff} L\right) m_P v_0 \sigma_b a^2}{4e\tau V_0}\right] \qquad (42)$$

Applying the relationship in equation (17) to equation (42) knowing that $V_0 = Z_C I = I\omega L_i$, with all symbols having meaning as defined before, we have

$$P_C = \frac{2\pi I^2 \omega^2 L_i^2 L_0}{\left(L_0^{\,2} + 2L_0 kL + L^2 K^2\right)}\left[\frac{\sigma_b a^2}{2} + \frac{\sigma_t R^2}{2} + \frac{\left(L_0 + k_{eff} L\right) m_P v_0 \sigma_b a^2}{4e\tau V_0}\right] \qquad (43)$$

Equation (43) defines the electrostatic Coulomb power loss of both the patient tissue with the contribution of flowing blood in the vessels.

5.0 Analysis Of Result and Conclusion

Equations (36) and (43) have been used to compute the P_f and P_C respectively of the human tissue using the conductivity of blood as 0.0054 mho with patient tissue length of 0.02 m and the proximity of the patient to the capacity (L), varying from 0.005 m to 0.0020m. The result is shown in Table 1 (a). The ratio of P_C/P_f as calculated is also given in the same table. When the tissue proximity to the capacitor is 0.005 m, P_C/P_f is 0.05 but becomes 0.54 at L = 0.002 m at the same tissue length.

Awojoyogbe [17] in his model (considering no contribution due flowing blood) carried out a calculation of PC/P_f using the values of L_0 and L. His results are presented in Table 1 (b). In comparison, his values of P_C/P_f are seen to be quite higher than those obtained from our present model with percentage variation as high as 81% (Table 2) in the set L_0 = 0.02 m and L = 0.005m.

Significantly, the performance of NMR instrument as explained earlier requires that the value P_C/P_f be sufficiently low for a good performance and minimal power loss. The present result therefore indicates that the estimation of rF absorption in human subject has to some extent something do with flowing blood in the tissue and so be taken into consideration in NMR instrument design for purpose of accurate medical diagnosis especially at low frequencies. The calculation presented here show that blood flow contributes to P_f and P_C which hitherto has not been considered an important factor.

The problems of power dissipation and temperature variation in biological tissue during microwave blood perfusion and other activities outside NMR have been given adequate treatment by other researchers [19-23].

Table 1 Values of P_C/P_f calculated with our present equations (equations 36 and 43) and those of Awojoyogbe [17] respectively.

L_0 (m)	L (m)	L_0/L	P_C/P_f (Present values)	P_C/P_f (Awojoyogbe)
0.02	0.0050	4.0	0.04	0.22
0.02	0.0030	4.7	0.43	0.66
0.02	0.0025	8.0	0.48	0.97
0.02	0.0020	10.0	0.54	1.50

Table 2 Comparison of P_C/P_f values calculated by Awojoyogbe [17] with those based on our present equations (36) and (43)

L_0 (m)	L (m)	L_0/L	P_C/P_f (Awojoyogbe)	P_C/P_f (Present values)	Percentage Deviation
0.02	0.0050	4.0	0.22	0.04	81
0.02	0.0030	4.7	0.66	0.43	65
0.02	0.0025	8.0	0.97	0.48	49
0.02	0.0020	10.0	1.50	0.54	36

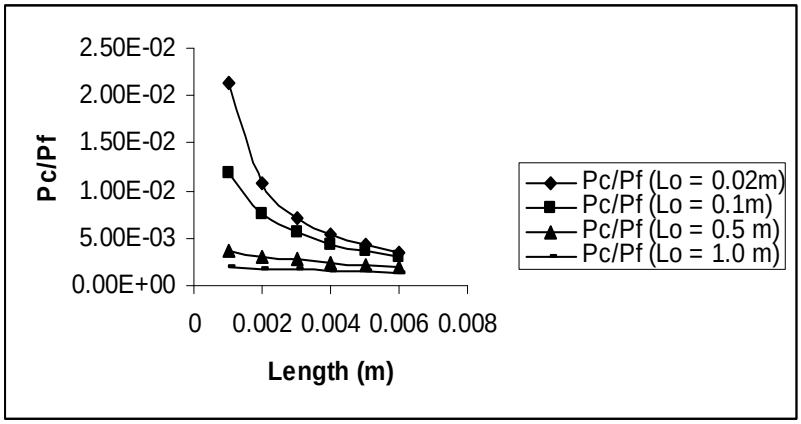

Fig. 5 Graph of P_C/P_f against the proximity of the Patient to the Capacitor plate (L) such that L varies from 0.001 m to 0.006 m where the lengths of patient are taken from 0.02 m to 1.0 m. The conductivity patient is taken as 0.4 s/m while that of blood is taken as 0.0054 s/m; the dielectric constant of the tissue K_{eff} = 100 and the angular frequency is 6.28×10^7 rad/sec. The axial blood velocity is 10 m/s

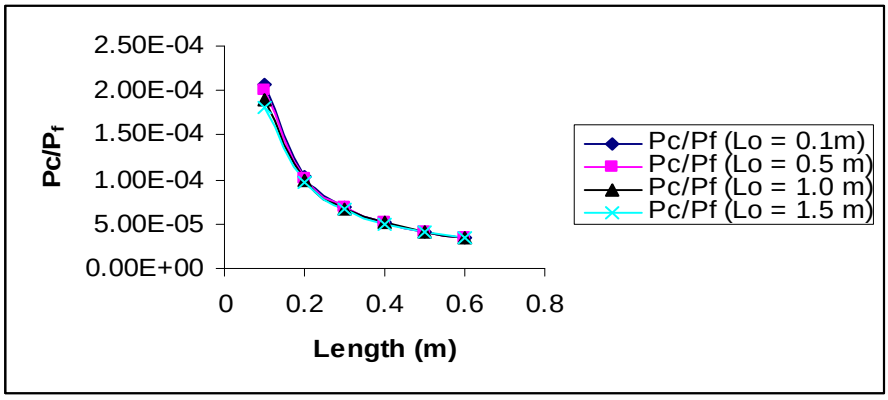

Fig. 6 Graph of P_C/P_f against the proximity of the Patient to the Capacitor plate (L) such that L varies from 0.1 m to 0.6 m where the lengths of patient are taken from 0.02 m to 1.0 m. The conductivity patient taken as 0.4 s/m while that of blood taken as 0.0054 s/m; the dielectric constant of the tissue K_{eff} = 100 and the angular frequency is 6.28×10^7 rad/sec. The axial blood velocity is 10 m/s.

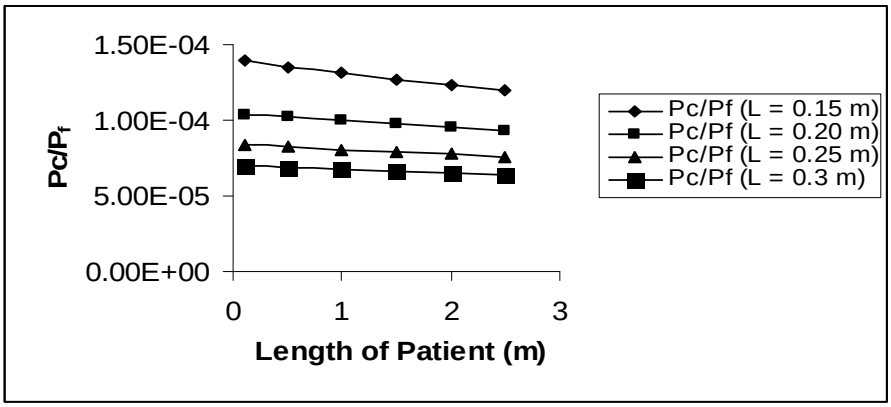

Fig. 7 Graph of PC/Pf against length of patient (L0) such that L0 varies from 0.1 m to 2.5 m where the proximity of the patient to the capacitor (L) for the four graphs 0.10m, 0.20m, 0.25m and 0.30 m. The conductivity patient is taken as 0.4 s/m while that of blood is taken as 0.0054 s/m; the dielectric constant of the tissue Keff = 100 and the angular frequency is 6.28 × 107 rad/sec. The axial blood velocity is 10 m/s.

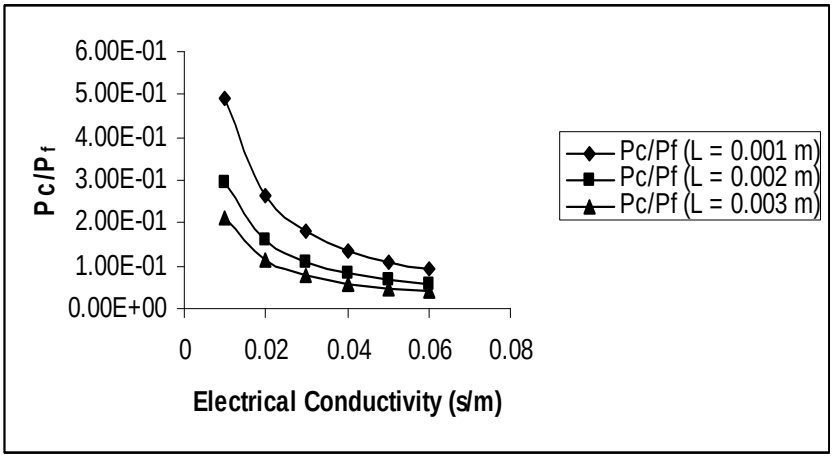

Fig. 8 Graph of P_C/P_f against conductivity of patient (σ_t) such that (σ_t) varies from 0.01 s/m to 0.06 s/m while the blood conductivity is (σ_b) 0.0054 s/m. The proximity of the patient to the capacitor plate (L) for the three graphs are 0.001 m, 0.002 m and 0.003 m while the length of the patient (L_0) is 0.05 m; the dielectric constant of the tissue is 100 and the angular frequency ω is 6.28 x 10^7 rad/sec. The axial blood velocity is 10 m/s.

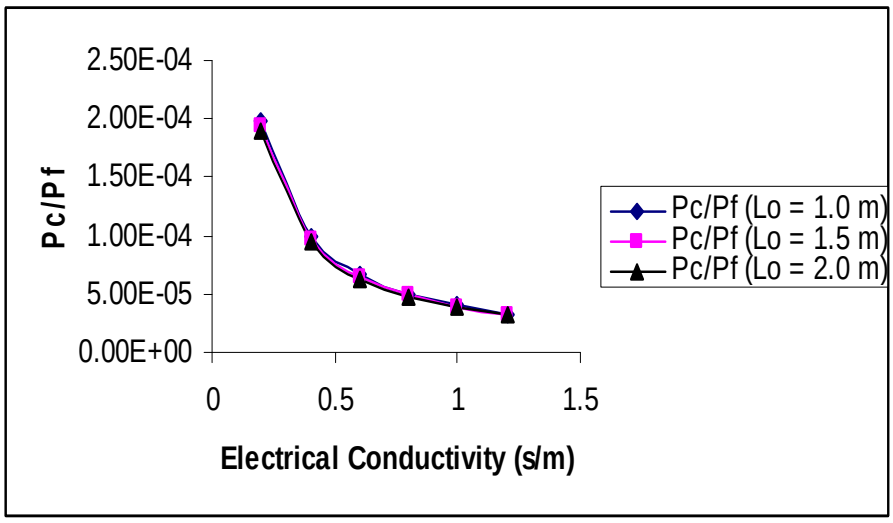

Fig. 9 Graph of Pc/P_f against conductivity (σ_t) such that (σ_t) varies from 0.2 s/m to 1.2 s/m while the blood conductivity is 0.0054 s/m. The length of the patient (L_0) for the three graphs 1.0 m, 1.5 m and 2.0 m while the proximity of the patient to the capacitor (L) is 0.2 m; the dielectric constant of the tissue K is 100 and the angular frequency ω is 6.28 x 10^7 rad/sec. The axial blood velocity is 10 m/s.

References

[1] Bottomley, P.A. and Roemer, P.B. (1992), Homogeneous Tissue Model Estimates of rF Power Deposition in Human NMR Studies. *Annals of the New York Academy of Sciences*. **649**(1): 144-159.
[2] Adair, E.R. and Berglund, L.G. (1988), Thermoregulatory Consequences of NMR Imaging. *Reson. Imaging***4**: 321-333.
[3] Adair, E.R. and Berglund, L.G. (1988), Thermoregulatory Consequences of NMR Imaging when Capacity for Skin Blood Flow is Reduced. Abstract, Society for Magnetic Resonance in medicine, pp 171.
[4] Adair, E.R. and Berglund, L.G. (1989), Thermoregulatory Consequences of Cardiovascular impairment during NMR Imaging in Warm/Humid Environments. *Magn Reson. Imaging***7**:25-37.
[5] Adair, E.R. and Berglund, L.G. (1992), Predicted Thermophysiological Responses of Humans to MRI field. In Margin, R.I.; Liuburdy, R.P. and Person B ads. Biological Effects and Safety aspects of Nuclear Magnetic Resonance imaging and Spectroscopy. *Annals of the New YorkAcademy of Sciences***649**:188-200.
[6] De, D.K and Moran, P.R. (1988), World Congress in Medical Physics and Biomedical Engineering, 6-12 August, San Antonio, Texas, USA.
[7] Bottomley. P.A. and Edelstein, W.A. (1981), Power Deposition and in Whole-body NMR Imaging. *Med. Phys.* **8**: 510-512.
[8] Athey, T.W. (1989), A Model of the temperature Rise in the Head due to Magnetic Resonance Imaging Procedures. *Magn Reson Med***9**:177-184.
[9] Collins. C.M.; Li, S. and Smith, M.B. (1998), SAR and B_1 field Distribution in a Heterogeneous human Head model within a Birdcage Coil. *Magnetic resonance in Medicine***40**; 6, 847.
[10] Van den Bergh, A,J.; ven den Booget, H.J. and Heerchap, A. (1998), calibration of 1H Decoupling field Strength and Experimental Evaluation of the Specific RF Absorption Rate in 1 H-decoupled Human C-MRS. *Magnetic Resonance in Medicine***39**; 4, 189.
[11] Hand, J.W.; Lau, R.W.; Lagendjik, J.J.W.; Ling, J.; Burl, M. and Young R.I. (1999), Electromagnetic and Thermal Modelling of ASR and Temperature Fields in Tissue Due to an RF Decoupling Coil. *Magnetic Resonance in Medicine***42**: 1, 183.
[12] Macdonald, J.M.; Schmidlin, O. and James, T.L. (2002), In vivo monitoring of Hepatic Glutathione in Anaesthetizes Rats by 13C NMR. *Magnetic Resonance in Medicine***48**: 3, 40.
[13] Prock, T.; Collins, D.J. and Leach, M.O. (2002), A model to Assess SAR for Surface coil Magnetic Resonance Spectroscopy Measurements. *Physics in Medicine and Biology***47**: 10, 1805.
[14] Kay, L.; Shimoide, K. and Freeman, W.J. (1996), Comparison of EGG Time Series from Rat Olfactory System with Model Composed of Coupled Oscillators. *Intern Journ of Bifurcation and Chaos*. **5**(3): 849-858.
[15] Peters, M.J.; Stinstra, G. and Hendriks, M. (2001), Estimation of the Electrical conductivity of Human Tissue. *Electromagnetics*, Vol **21**(7-8): 545-557.
[16] Hoetink, A.E.; Faes, T.J.C.; Visser. K.R. and Heethaar, R.M. (2004), On the flow Dependency of the Electrical Conductivity of Blood. *Biomedical EngineeringTransaction, IEEE Transaction*. Vol. **51**(7): 1251-1261.
[17] Awojoyogbe, O.B. (1997), "Studies on the Application of Nuclear Magnetic Resonance (NMR, MRI) in the Estimation of Human Blood Flow Rates". Ph.D Thesis, Federal University of Technology, Minna, Nigeria. (Unpublished).
[18] Vermeulen, F.E. and Chute, F.S. (1983), *Can. Elec. Eng*.**8**(3) 93-99.
[19] Liu, J. (2000), Preliminary Survey on the Echaniss of the Wave Like Behaviors of Heat Transfer in Living Tissue. *Forschung Im Ingenieuwesen springer- Verlag*, **66**: 1-10.
[20] Ozen, S,; Colekci, M. and Merdan, M. (2000), "Over Exposure of Electric and Magnetic Field for Patient and Operators from RF Diathermy Experiment", Isik Workshop on Biomedical Information Engineering, IsikUniversity, Istanbul, Turkey, 190-192.
[21] El-dabe, N.T.; Mona, A.A.M. and El-sayed, F. (2003), Effects of Microwave Heating on the Thermal States of Biological tissues. *Afr. J. Biotechnol*., 453-459.
[22] Adebile, E.A.; Ayeni, R.O. and Aregbesola, Y.A.S. (2005), Steady-stateTemperaturein Biological Tissues Undergoing Microwave Hyperthermic. *Int. J. Biol Phys. Sci. Focus*. 101-108.
[23] Adebile, E.A.; Akintewe, B.N. and Ogunmoyela, J.K. (2007), Temperature Variation in Biological Tissues Due to Spatial Dependent Blood Perfusion During Microwave Heating. *J. Eng. Applied Sci*., **2** (3): 509-515.